

2010

A Microscale Monolithic Absorption Heat Pump

Matthew D. Determan
Georgia Institute of Technology

Srinivas Garimella
Georgia Institute of Technology

Follow this and additional works at: <http://docs.lib.purdue.edu/iracc>

Determan, Matthew D. and Garimella, Srinivas, "A Microscale Monolithic Absorption Heat Pump" (2010). *International Refrigeration and Air Conditioning Conference*. Paper 1156.
<http://docs.lib.purdue.edu/iracc/1156>

This document has been made available through Purdue e-Pubs, a service of the Purdue University Libraries. Please contact epubs@purdue.edu for additional information.

Complete proceedings may be acquired in print and on CD-ROM directly from the Ray W. Herrick Laboratories at <https://engineering.purdue.edu/Herrick/Events/orderlit.html>

A Microscale Monolithic Absorption Heat Pump

Matthew D. Determan, Srinivas Garimella*

Sustainable Thermal Systems Laboratory
George W. Woodruff School of Mechanical Engineering
Georgia Institute of Technology
Atlanta, GA
(404) 894-7479; srinivas.garimella@me.gatech.edu

* Corresponding Author

ABSTRACT

A comprehensive development of a miniaturized thermally activated cooling system is reported here. This study represents the first ever conceptualization, design, fabrication and successful experimental demonstration of a thermally activated microscale absorption heat pump for miniaturized or mobile applications. A 300 W nominal cooling capacity ammonia-water absorption heat pump with overall dimensions of $200 \times 200 \times 34$ mm and a mass of 7 kg was fabricated and successfully tested over a range of heat sink temperatures from 20 to 35°C and desorber thermal input rates ranging from 500 to 800 W. Measured evaporator coolant heat duties ranged from 136 to 300 W, while system COPs ranged from 0.247 to 0.434. At a nominal rating condition of 35°C heat sink temperature, the maximum thermal input of 800 W produced a cooling effect of 230 W, representing a COP of 0.29.

1 INTRODUCTION

Thermally activated systems have the ability to produce useful cooling from waste heat streams such as engine exhaust or directly from the combustion of liquid fuels. Applications that could benefit from miniaturization of absorption system technology include waste heat recovery and upgrade for heat-driven chillers and heating and air-conditioning systems, water heating and cogeneration systems, vehicular, marine and refrigerated transport of food, medicines, vaccines, and other perishable items.

Few concepts for miniaturized or mobile, thermally activated cooling systems exist in the literature, and even in such cases, successful fabrication and testing has been elusive. Gryzll and Balderson (1997) developed a 19.9 kg adsorption system using a calcium oxide that provided 150 W for 4 hrs. Rahman (1996) investigated the use of a Brayton cycle to provide mobile cooling for soldiers. The system was estimated to have dimensions of $0.47 \times 0.279 \times 0.368$ m. No estimate of the mass of the system was given. No prototype was developed in this study, and no experimental results were presented. Salim (2004) proposed a thermally activated mobile ejector refrigeration system for use in automobile cooling. The system used waste heat from the engine coolant at 90°C, and from the exhaust gas (220 – 990°C depending on driving conditions) to drive the refrigeration cycle. A high pressure vapor stream is expanded through a convergent-divergent nozzle to induce a secondary flow of refrigerant from the evaporator. While the system still requires power to drive a pump, it is a small fraction of the power required to drive the compressor in current automobile vapor compression systems. A thermodynamic model of the proposed system was described and COPs of 0.5-1.04 were predicted for several heat input methods. However, in this case also, experimental results were not reported. Wang *et al.* (2004) analyzed a combination of a Rankine power cycle and a vapor compression cycle for use as a portable cooling system. The high COP of the vapor compression cycle is utilized while also taking advantage of the heat-actuation provide by the incorporation of a Rankine power cycle.

Ernst and Garimella (2007; 2008; 2009) designed and fabricated a vapor compression refrigeration system for completely autonomous mobile cooling of an individual. The cooling system was driven by a miniature internal combustion engine linked to a miniature reciprocating piston compressor. The working fluid was R-134a. The condenser was an air-coupled aluminum microchannel heat exchanger. The evaporator was integrated into a vest to provide cooling to the torso of an individual. The system provided a cooling capacity of 230 W at an ambient

temperature of 43.3°C with an overall, fuel-to-cooling efficiency of 10.2%. The 4.4 kg system with a fuel supply of 1.8 kg would be able to provide the cooling capacity stated above for 5.7 hours. The exhaust gases and noise generated from the small internal combustion engine are drawbacks of this technology.

Drost (1999) described a man-portable absorption heat pump for use as a microclimate cooling system. The proposed cooling system was a single-effect water/lithium bromide absorption heat pump with a water cooled absorber and condenser. One of the systems described would use a thermoelectric device to provide some of the required electrical power. The potential performance of the various components was discussed and an estimate of 4 to 5 kg in an envelope of $20 \times 22 \times 8$ cm was given for a system with a 350 W cooling capacity. It is not clear, however, whether this system was ever successfully fabricated as no experimental results were presented.

In the present study, a miniaturized monolithic heat pump is fabricated by bonding multiple sheets of thin metal, each with fluid channels and headers, to form the numerous components of an absorption heat pump. The channels are formed in the sheets using a photo-chemical etching process and the multiple sheets are joined together by a diffusion bonding process. This concept allows all of the heat and mass exchangers to be fabricated in a single manufacturing process, resulting in a system with internal fluid coupling between components, substantially reducing the risk of leakage. Figure 1 shows a drawing of the stacked sheets that form the core of the heat exchangers. The pictured component is the absorber. The dilute solution liquid enters the microchannel from the square header, while the refrigerant vapor enters from the circular header in the lower right. The vapor is then distributed to all of the channels and introduced into the solution channel via small orifices. The coolant, which is flowing on the shim below the top-most sheet visible in this image, exits via the circular header in the upper left corner. Figure 2 shows several views of the internal components of the monolithic device.

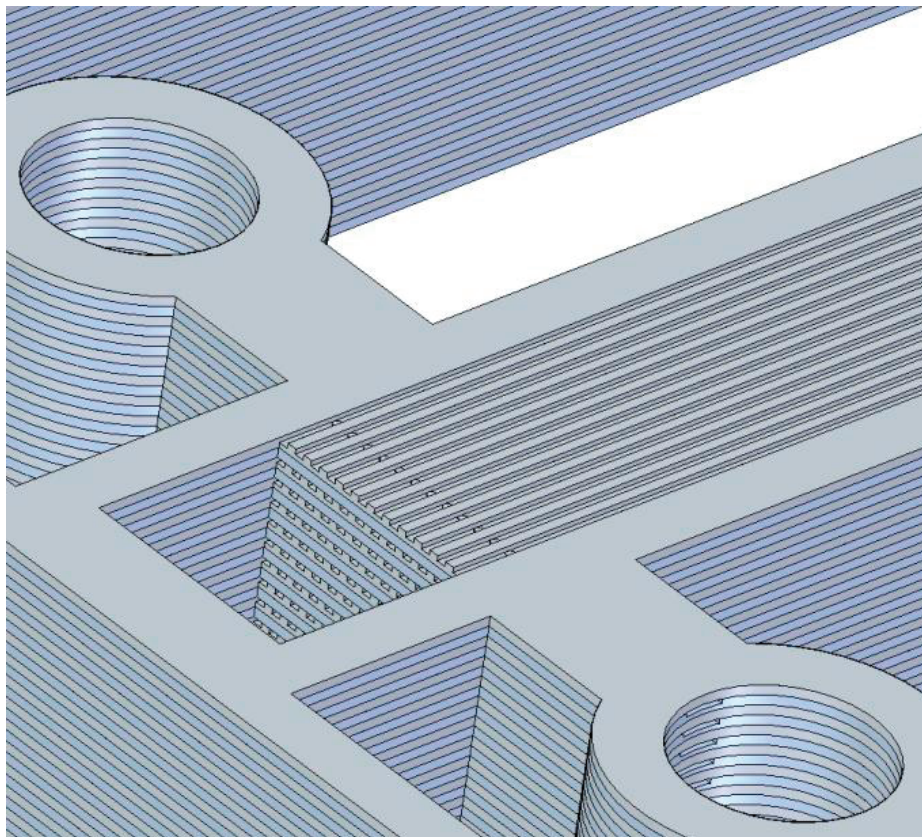


Figure 1: Drawing of stack of sheets forming the core of a microchannel heat and mass exchanger

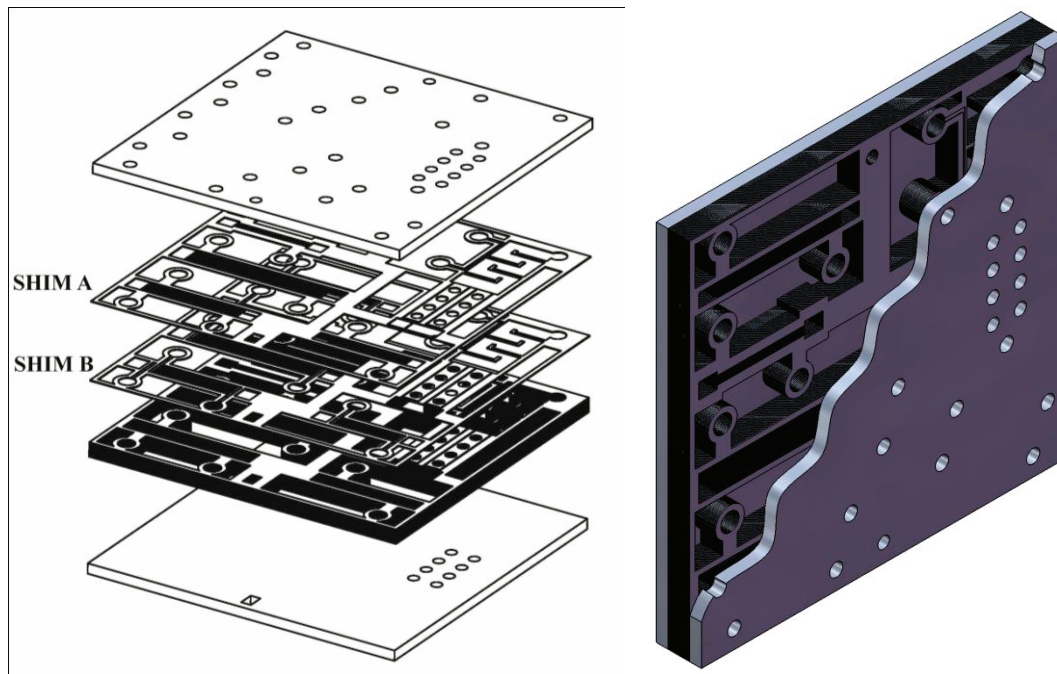


Figure 2: Internal Views of Microscale Monolithic Absorption Heat pump

2 SYSTEM DESIGN

A thermodynamic cycle model of a single-effect ammonia-water absorption cycle was developed using *Engineering Equation Solver* (EES) software (Klein 2009) to estimate the required component sizes for the microchannel system. This model established the operating conditions of the experimental system. To fully describe the operating conditions, several input variables and assumptions about the state of the working fluids are required. The operating pressures and concentrations at various locations in the cycle are dictated by mass and species balances, the ambient temperature and the heat exchange performance of the various components. The design point for the system was an ultimate heat sink temperature of 37°C and a thermal power input of 800 W. For the design point calculation, the concentrated solution mass flow rate was set to 2.7×10^{-3} kg/s with an ammonia mass fraction of 0.37. The flow rates and concentration were based on the desired cooling capacity of 300 W and the ambient and heat source temperatures. The refrigerant vapor outlet from the rectifier was assumed to be at a saturated vapor state, while the dilute solution outlet from the desorber was assumed to be at a saturated liquid state. The state of the reflux was determined by assuming that it is a saturated liquid. This model was used to estimate the required heat exchanger UA and then the actual heat exchanger physical sizes. Figure 3 shows the layout of the components on shim A. The components are separated from each other by voids to provide a thermal break to reduce parasitic heat conduction between components as well as to reduce the weight of the system.

A shim thickness of 0.5 mm was chosen. With a channel etch depth of half the shim thickness and a channel width of 0.5 mm, the nominal channel hydraulic diameter for this prototype is 306 μm , with a channel horizontal transverse pitch of 1 mm and vertical pitch of 0.5 mm. The channels are formed by a chemical etching process. A photosensitive material was applied to either side of the stainless steel shims, then a mask containing the image of the channel geometry is positioned over the shim and the entire assembly is exposed to UV light. Following the UV exposure, the uncured photosensitive material is removed, exposing the steel below.

The sheet is then passed through an acid bath. The acid attacks the exposed steel, creating the microchannels. The monolithic assembly is created by stacking the shims in alternating layers, between two end plates that contain the required fluid inlet and outlet connections. The system contained a total of 40 shims, 20 of shim A and 20 of shim B. The entire stack was then diffusion bonded, creating a hermetically sealed system that contains all of the heat and mass exchangers for the heat pump system. Figure 4 illustrates the dimensions of the monolithic heat pump system. The system has exterior dimensions of $200 \times 200 \times 34$ mm and a mass of 7 kg.

3 SYSTEM TESTING

The test facility with the monolithic absorption heat pump installed is shown in Figure 5. The numerous external fluid inlet and outlets were required to provide access for instrumentation. The solution pump was a variable speed, magnetically coupled gear pump. Eight 150 Watt electrical resistance cartridge heaters provided the thermal energy input to the desorber. The heaters were controlled by a manual variable voltage transformer. This arrangement allowed for precise control and measurement of heat input rates from 0-1200 W. The heaters and the inside of the heater holes were covered with a thermally conductive paste to ensure good thermal contact between the heaters and the shims. During testing, the system and the connecting plumbing were insulated to reduce heat loss to the ambient.

All thermocouple measurements were made with type T thermocouples, which have an uncertainty of $\pm 0.5^\circ\text{C}$. The pressure measurements were made with WIKA pressure transducers (ECO-1, $\pm 0.5\%$ of span). Solution flow rates were measured with DEA Engineering Company flow meters (FMTE20, $\pm 0.5\%$ of reading). The power input to

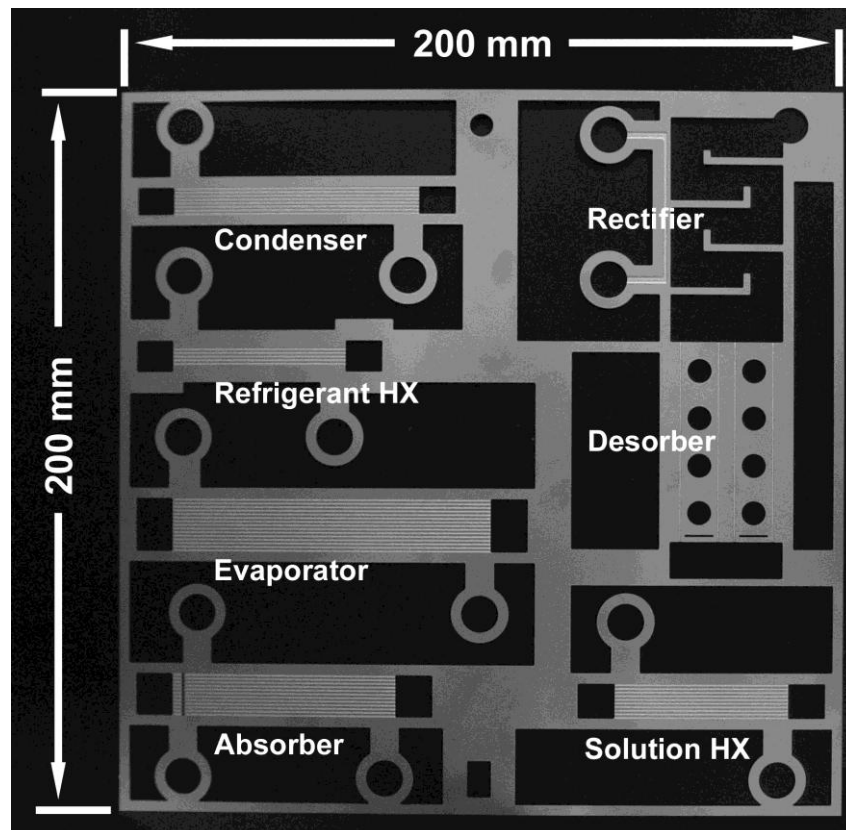


Figure 3: Individual Components on Shim A

the generator was measured with an Ohio Semitronics wattmeter, (PC5-019E, $\pm 0.5\%$ F.S.). The water coolant flow rates were measured with Key Instruments flow meters (MR3000, $\pm 4.0\%$ F.S.). All voltage signal measurements were recorded with a National Instruments SCXI signal conditioning and data acquisition system. Two SCXI-1102 modules, each with 32 channels, were housed in a SCXI-1000 chassis. Electrical connections were made to the SCXI-1102 modules via SCXI-1303 isothermal terminal blocks with a built in reference junction for cold-junction compensation of thermocouple measurements. The signal conditioning system was connected to a PC via a DAQCard-6036E data acquisition card. Frequency measurements were recorded with an IOTech Personal DAQ/56 data acquisition system connected to a personal computer via USB. Both the National Instruments and the IOTech data acquisition systems were controlled with LabVIEW.

An analysis of a single test point is presented here for illustration of the data reduction. The uncertainty propagation is calculated using the procedure of Taylor and Kuyatt (1994). The calculations were conducted using the built-in error propagation utilities in EES (Klein 2009). The properties of water and ammonia/water mixtures supplied with EES were used for these calculations. The absorber coolant inlet temperature for this test point was $30.2 \pm 0.5^\circ\text{C}$ and the electrical input to the desorber heaters was 708.9 ± 7.5 W. The dilute solution leaving the rectifier was at a saturated condition at a temperature of $115.4 \pm 0.5^\circ\text{C}$. The system high-side pressure was 1304 ± 17.4 kPa. Based on these measured quantities, the calculated concentration of the dilute solution was 0.299 ± 0.003 . The measured dilute solution volumetric flowrate was 64.8 ± 0.3 ml/min. The dilute solution density, based on the dilute solution concentration, system high side pressure, and the solution heat exchanger outlet temperature of $47.7 \pm 0.5^\circ\text{C}$, was 880.8 ± 1.2 kg/m³. This yields a dilute solution mass flowrate of $9.51 \times 10^{-4} \pm 4.9 \times 10^{-6}$ kg/s.

The refrigerant vapor temperature leaving the rectifier was $102.2 \pm 0.5^\circ\text{C}$. At this saturated vapor condition, the refrigerant mass concentration was calculated to be 0.946 ± 0.002 . The concentrated solution volumetric flowrate was 88.2 ± 0.4 ml/min. The temperature of the concentrated solution inlet to the solution heat exchanger was $36.3 \pm 0.5^\circ\text{C}$, the system high side pressure was 1304 ± 17.4 kPa, and the density was calculated to be 838.4 ± 1.5 kg/m³. This yields a concentrated solution mass flowrate of $1.23 \times 10^{-3} \pm 5.4 \times 10^{-6}$ kg/s. A mass and species balance on the solution circuit yielded a refrigerant mass flowrate of $2.8 \times 10^{-4} \pm 6.2 \times 10^{-6}$ kg/s and a concentrated solution concentration of 0.447 ± 0.004 . The evaporator refrigerant inlet temperature and pressure were $-1.3 \pm 0.5^\circ\text{C}$ and

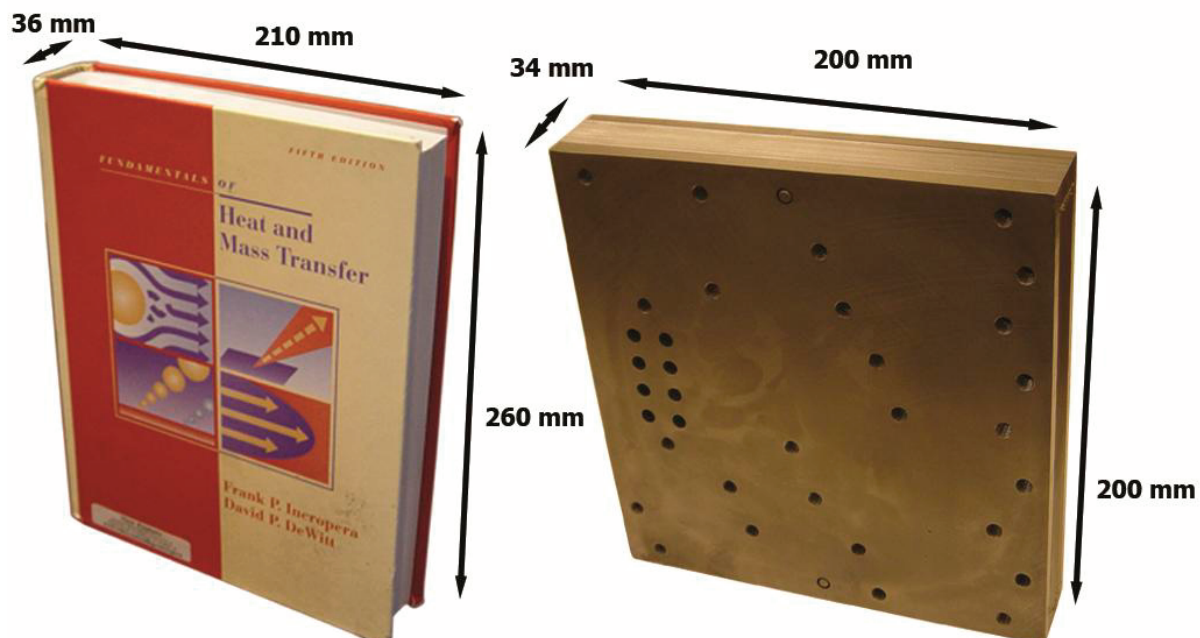


Figure 4: As Fabricated Microscale Monolithic Absorption Heat Pump

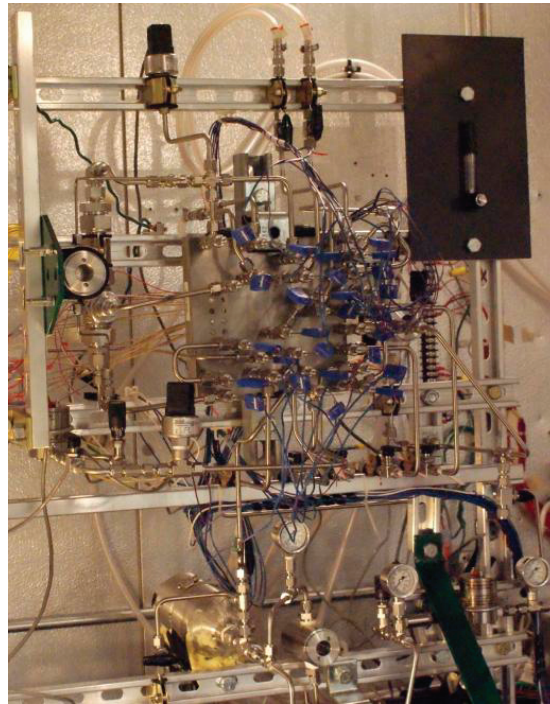


Figure 5: Monolithic Heat Pump in Test Facility

375.3±3.45 kPa, respectively. The calculated evaporator inlet enthalpy was 510.1±169.8 kJ/kg. The evaporator outlet refrigerant temperature was 16.8±0.5°C and the enthalpy, based on the pressure, temperature and concentration, was 1115±7.2 kJ/kg. (The refrigerant outlet temperature in this instance is greater than the evaporator chilled water inlet temperature due to local internal conduction from the desorber through the internal support structures of the system.) The refrigerant flow rate and the evaporator inlet and outlet enthalpies were used to calculate the refrigerant evaporator heat duty of 170±48 W. The uncertainty in this heat duty is large due to the small variation in temperature with enthalpy for low quality ammonia/water mixtures. An alternative method to calculate the refrigerant heat duty is to use the enthalpy of the refrigerant before the expansion valve and assume an isenthalpic expansion. The refrigerant outlet temperature from the high pressure side of the refrigerant heat exchanger was 22.6±0.5°C, which corresponds to a refrigerant enthalpy of 66.4±2.7 kJ/kg. Using this in place of the evaporator inlet condition, the evaporator refrigerant heat duty was calculated to be 295±7 W. This calculation has a much lower uncertainty due to the difference in slope of the enthalpy versus temperature relationship of a sub-cooled liquid and a low quality, high concentration, two-phase mixture of ammonia and water. It does not take into account any losses in the expansion process or heat gains through the tubing between the expansion valve and the inlet of the evaporator. The measured evaporator chilled water flow rate was 631±101 mL/min. The chilled water inlet temperature was 12.5±0.5°C, at which the density is 999.4±0.1 kg/m³, resulting in a chilled water mass flow rate of 10.5×10⁻³±1.7×10⁻³ kg/s. The chilled water outlet temperature was 7.1±0.5°C. The corresponding chilled water inlet and outlet enthalpies were 52.8±2.1 kJ/kg and 30.1±2.1 kJ/kg respectively. This results in a calculated evaporator chilled water heat duty of 239±49 W. The difference between the calculated chilled water heat duty and the refrigerant evaporator heat duty calculated using the refrigerant state at the inlet of the expansion valve was 56 W or 23% of the water-side heat duty. To calculate a system COP, the water-side heat duty was used. Given the uncertainty in the refrigerant-side calculations as well as the heat losses and gains to the system and the internal conduction issues, the water-side calculations were considered more appropriate for indicating system performance. The water-side heat duty also represents the useful amount of cooling that the system produced. Using the evaporator chilled water heat duty, the system COP was calculated as 0.34±0.07. At a standard chiller rating condition of 35°C heat sink temperature, the monolithic system delivered a cooling duty of 230 W, and was able to deliver a cooling load of 300 W with a heat sink of 20°C.

4 CONCLUSIONS

In the present work, a versatile, modular, scalable design for miniaturized absorption heat pumps was developed. Alternating plates photo-etched with working fluid and coupling fluid channels for all components of a single-effect absorption heat pump were stacked and diffusion bonded to form the entire absorption system assembly in monolithic fashion. In the present first-of-a-kind, proof-of-concept design with a focus on demonstrating feasibility rather than maximized performance, the use of a coflow design of the desorber, and suboptimal thermal contact between coolant and vapor in the rectifier resulted in relatively low COPs. Analysis of the data indicated that improved desorber and rectifier designs to increase refrigerant generation and purity would yield substantial improvements in cooling capacity as well as system COP, while maintaining a small device footprint. Furthermore, improved designs to reduce parasitic heat conduction between components within the system will also yield significant performance improvements. It is estimated that a system similar in configuration to the one in this study, but with all fluid connections internal to the system, and without instrumentation required for system validation, would achieve the same cooling capacity with a system mass of 2.5 to 3.5 kg in an envelope of $120 \times 120 \times 25$ mm. Thus, this study conclusively demonstrates that the utilization of microscale fluid flow and heat and mass transfer principles enables the realization of compact thermally activated heat pump packages that deliver cooling and heating in substantially smaller system footprints and volumes than the state of the art. The modular design of the system enables the utilization of a wide range of source energy temperatures for a wide range of cooling and heating loads and temperatures. Waste heat recovery and upgrade for heat-driven chillers and heating and air-conditioning systems, water heating and cogeneration systems, vehicular, marine and refrigerated transport of food, medicines, vaccines, and other perishable items are among the applications that could benefit from the absorption system technology developed and reported here.

REFERENCES

- Drost, K. (1999), "Mesoscopic Heat-Actuated Heat Pump Development," *American Society of Mechanical Engineers, Advanced Energy Systems Division (Publication) AES*, 39: 9-14.
- Ernst, T. C. and Garimella, S. (2007), "Wearable Engine-Driven Vapor-Compression Cooling System for Elevated Ambients," *IMECE, November 11-15, 2007, Seattle, WA, IMECE2007-43734*, Seattle, WA
- Ernst, T. C. and Garimella, S. (2008), "Demonstration of a Wearable Cooling System for Elevated Ambient Temperature Duty Personnel," *Proc. 19th National & 8th ISHMT-ASME Heat and Mass Transfer Conference, January 3 - 5, 2008, Hyderabad, India, , SPH-6*.
- Ernst, T. C. and Garimella, S. (2009), "Wearable Engine-Driven Vapor-Compression Cooling System for Elevated Ambients," *Journal of Thermal Science and Engineering Applications*, 1 (2): 025001-10.
- Grzyll, L. R. and Balderson, W. C. (1997), "Development of a Man-Portable Microclimate Adsorption Cooling Device, Honolulu, HI, USA, IEEE, Piscataway, NJ, USA, pp. 1646-1651.
- Klein, S. A. (2009). Engineering Equation Solver, F-Chart Software.
- Rahman, M. M. (1996), "Analysis and design of an air-cycle microclimate cooling device," *Transactions of the ASME. Journal of Energy Resources Technology*, 118 (4): 293-9.
- Salim, M. (2004), "Thermally Activated Mobile Ejector Refrigeration System Analysis," *Proceedings of the Institution of Mechanical Engineers, Part D: Journal of Automobile Engineering*, 218 (9): 1055-1061.
- Taylor, B. N. and Kuyatt, C. E. (1994). Guidelines for Evaluating and Expressing the Uncertainty of NIST Measurement Results. National Institute of Standards and Technology Technical Note 1297.
- Wang, H., Drost, K. and Peterson, R. (2004), "Thermodynamic Performance of a Miniature Expander/Compressor Heat-Actuated Heat Pump," *2nd International Energy Conversion Engineering Conference*, Providence, RI, United States, American Institute of Aeronautics and Astronautics Inc., Reston, VA 20191, United States, pp. 1455-1461.